INSTITUT DE FRANCE
Académie des sciences

Comptes Rendus

Géoscience

Sciences de la Planète

Milan Stafford Tchouatcha, Arnaud Patrice Kouske, Primus Azinwi Tamfuh, Alain Préat, René Toyama, Roger Feumba, Vannelle Tiokeng Ngounfack, Vivant Madjingain, Yaya Berinyuy Konglim and Rigobert Tchameni

First evidence of sinter and travertine in Cameroon: fault reactivation and geothermal implications

Volume 355 (2023), p. 279-298

Published online: 28 September 2023

https://doi.org/10.5802/crgeos.230

Les Comptes Rendus. Géoscience — Sciences de la Planète *sont membres du Centre Mersenne pour l'édition scientifique ouverte*
www.centre-mersenne.org
e-ISSN : 1778-7025

Comptes Rendus
Géoscience — Sciences de la Planète
2023, Vol. 355, p. 279-298
https://doi.org/10.5802/crgeos.230

Research article — Geochemistry, cosmochemistry

First evidence of sinter and travertine in Cameroon: fault reactivation and geothermal implications

Milan Stafford Tchouatcha *, [a], **Arnaud Patrice Kouske** [b], **Primus Azinwi Tamfuh** [c, d], **Alain Préat** [e], **René Toyama** [f], **Roger Feumba** [g], **Vannelle Tiokeng Ngounfack** [a], **Vivant Madjingain** [h], **Yaya Berinyuy Konglim** [a] and **Rigobert Tchameni** [h]

[a] Department of Earth Sciences, Faculty of Science, University of Dschang, P.O. Box 67, Dschang, Cameroon

[b] University Institute of Technology, University of Douala, P.O. Box 8698, Douala, Cameroon

[c] Department of Soil Science, Faculty of Agronomy and Agricultural Sciences, University of Dschang, P.O. Box 222, Dschang, Cameroon

[d] Department of Mining and Mineral Engineering, National Higher Polytechnic Institute, University of Bamenda, P.O. Box 39, Bambili, Cameroon

[e] Res. Grp. - Biogeochemistry and Modeling of the Earth System - Sedimentology and Basin Analysis, University of Brussels, Av. F-D Roosevelt 50, B-1050, Brussels, Belgium

[f] Department of Earth Sciences, Faculty of Science, University of Bangui, P.O. Box 908, Bangui, Central African Republic

[g] Department of Earth Sciences, Faculty of Science, University of Yaoundé I, P.O. Box 812, Yaoundé, Cameroon

[h] Department of Earth Sciences, Faculty of Science, University of Ngaoundéré, P.O. Box 454, Ngaoundéré, Cameroun

E-mails: inter_milanac@yahoo.fr (M. S. Tchouatcha), arnaudpatricek@gmail.com (A. P. Kouske), aprimus20@yahoo.co.uk (P. A. Tamfuh), alainpreat@icloud.com (A. Préat), toyamarene@gmail.com (R. Toyama), rfeumba2002@gmail.com (R. Feumba), ngounfackvanelle@gmail.com (V. T. Ngounfack), madjingainvivant@gmail.com (V. Madjingain), berinyuyyaya@gmail.com (Y. B. Konglim), rigotchameni@yahoo.fr (R. Tchameni)

Abstract. The Laopanga hot spring deposits along the "Cameroon Volcanic Line" (CVL) are distinctive in being both siliceous sinter and travertine, made up of immature amorphous silica and mainly calcite, and associated with detrital deposits such as claystone, sandstone and conglomerate. Their age range from Plio-Pleistocene to Actual. Sr concentrations (17 to 2304 ppm) suggest an enrichment by epithermal outflows. δ^{13}C and δ^{18}O values, ranging respectively from 1.5‰ to 2.9‰ V-PDB and −10.1‰ to −6‰ V-PDB, reflect a high temperature of the parent solution (40 °C) related to an elevated geothermal gradient. The europium anomalies values (Eu/Eu*: 0.54–1.78) indicate the temperature variation of precipitated deposits related to distance of the deep hot water flow. The chemical

* Corresponding author.

compositions of the lithofacies show the diversity of the spring deposits related to complex phenomena of internal migration of mineralized hot water and the tectonic controls during the Precambrian fault reactivations.

Keywords. Plio-pleistocene to actual, Cameroon volcanic line, Laopanga basin, Central Cameroon shear zone, Precambrian fault.

Manuscript received 11 November 2022, revised 26 March 2023 and 27 April 2023, accepted 25 July 2023.

1. Introduction

Numerous hot springs are located along the "Cameroon Volcanic Line" (CVL) which is a megastructure with oceanic and continental volcanic fabrics from Pagalu Island to Lake Tchad displaying a "swell and basin" structure [Tchoua, 1974, Tchuimegnie Ngongang et al., 2016]. Some of these hot springs have travertine deposits near or far from the water source as for the Bongongo (near Mount Cameroon) and the Ngol (near Mount Manengouba) springs [Le Maréchal, 1976, Tchoua, 1977, Bisse et al., 2018, Tchouatcha et al., 2018]. The study area (Figure 1) concerns a small-sized (<0.15 Km length) sedimentary basin with thermogenic depositions. The deposits are atypical and made up of an alternation of detrital (conglomerates, sandstones and claystones) and chemical (travertines and siliceous sinters) facies (Figure 2). The case of alternation of travertine and detrital deposits is also reported in southern Tunisia [Henchiri et al., 2017].

Travertines and sinters are typical hydrothermal deposits in geothermal fields, and like "CVL", they are usually associated with recent volcanic eruptions [Suh et al., 2003]. Two origins have been suggested for the travertine formation [Magnin et al., 1991, Pentecost and Viles, 1994, Pentecost, 2005, Ollivier et al., 2009]: (i) hydrothermal and (ii) fresh water or meteoric. Moreover, Pentecost [2005], Gandin and Capezzuoli [2008] and Capezzuoli et al. [2014] distinguish the travertine and tufa deposit, based on the following characteristics such as the precipitation water temperatures (high in for the travertine deposits and ambient for the tufa deposit), the fabric (mainly regularly bedded to fine laminated in the travertine deposits and mainly poorly bedded in the tufa deposits), the $\delta^{13}C$ values (−1 to +10 V-PDB for the travertine deposits and <0 V-PDB for the tufa deposits) or the primary porosity (generally low in the travertine deposits and high in the tufa deposits). Meanwhile, according to Della Porta et al. [2017a] travertine can be very porous indicating the complexity of the hot spring carbonate deposits nomenclature.

The CVL travertines have been subject of many studies that led to their deep origin [e.g. Bisse et al., 2018, Tchouatcha et al., 2018] from hot springs, [31–49 °C, Le Maréchal, 1976]. Chemical elements such as Li, Ba, Sr and Sr in the host spring waters are commonly associated with CO_2 ranging from 500 to 1050 mg/l [Le Maréchal, 1976]. The high temperature parent solution with $\delta^{18}O$ (−8.4‰ to −6.4‰ V-PDB) and $\delta^{13}C$ (0.4‰ to 0.5‰ V-PDB) values at Ngol, and $\delta^{18}O$ (−5.8‰ to −5.9‰ V-PDB) and $\delta^{13}C$ (1.1‰ to 2‰ V-PDB) values at Bongongo, belonging to the CVL, reflect a mixture of hydrothermal and meteoric fluids for the genesis of travertines [Bisse et al., 2018]. This suggests a mixture between inorganic CO_2 and soil CO_2 from plant respiration [e.g., Giustini et al., 2017]. The heavy mineral content of these deposits reveals that the deep fluids crossed varied types of rocks such as plutonic and metamorphic rocks [Tchouatcha et al., 2018]. Gastropods and leaves occurring in the travertines suggest present-day climate conditions [Tchouatcha et al., 2018]. Despite the genetic link between travertine deposits and climate is well established [Kronfeld et al., 1988, Osmond and Dabous, 2004, Weisrock et al., 2008, Toker et al., 2015, Berardi et al., 2016, Vignaroli et al., 2016, Mancini et al., 2021], tectonics can also be determinant [Faccenna et al., 2008, De Filippis et al., 2013a]. The link between travertines and active tectonics has been established [Tchouatcha et al., 2016, 2018] and well known elsewhere [Altunel and Hancock, 1993, Altunel and Karabacak, 2005, Mesci et al., 2008, Brogi et al., 2012, 2020, 2021a,b, De Filippis et al., 2013b, Kanellopoulos et al., 2017, Matera et al., 2021].

Sinter or siliceous hot spring deposits are surface chemical precipitates related to geothermal systems, they are largely produced in near-neutral pH alkali chloride fluids oversaturated with silica [Hamilton et al., 2019]. Fluid composition may evolve to form acid-sulfate (–chloride), or bicarbonate springs related to alkali chloride parent fluids that migrated

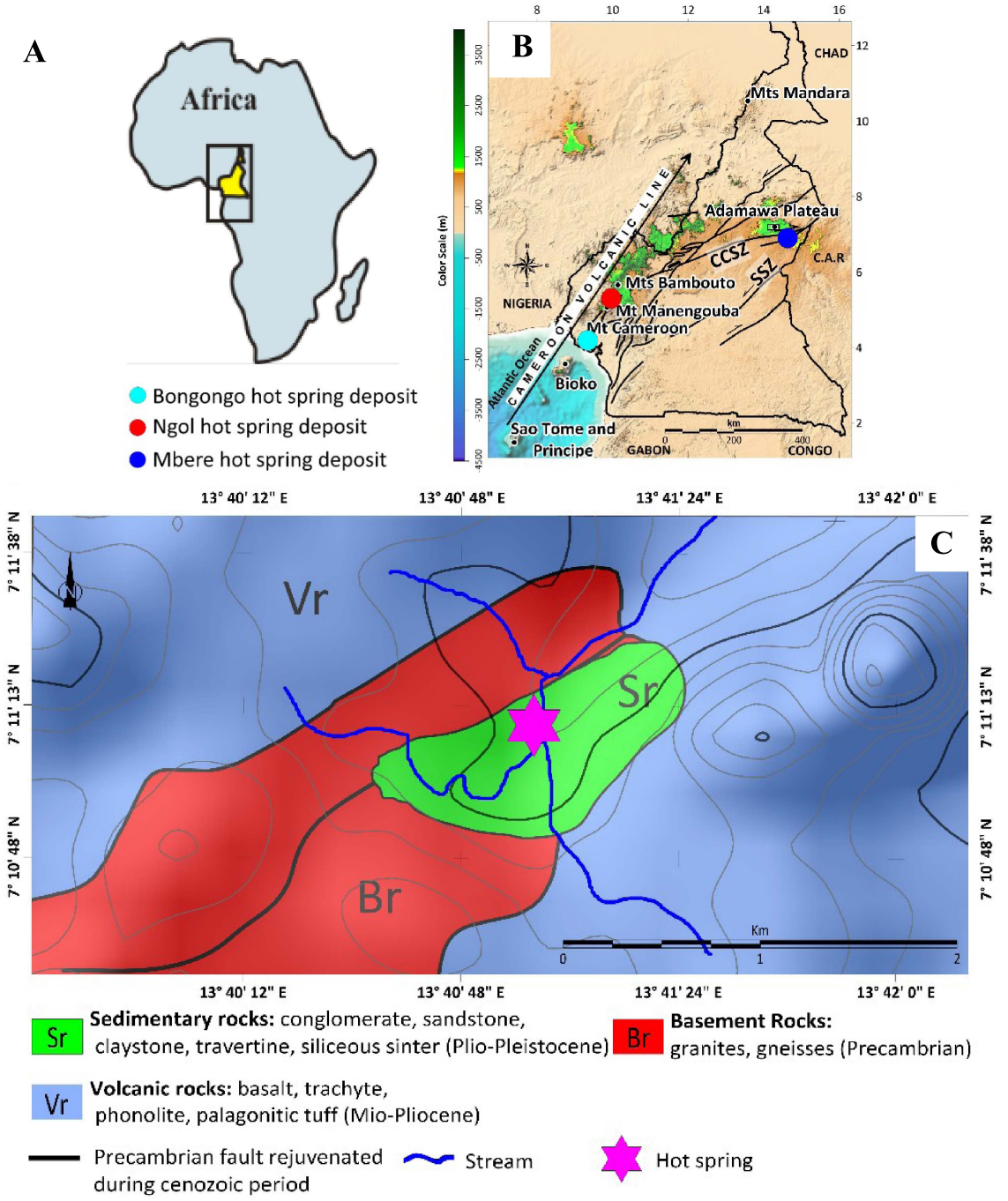

Figure 1. Geological context; (A) Location of the Cameroon map in Africa; (B) Location of the studied area in the Cameroon Volcanic Line. (C) Geological map of the studied area [modified from Lasserre, 1961, 1962, Temdjim et al., 2004, 2010].

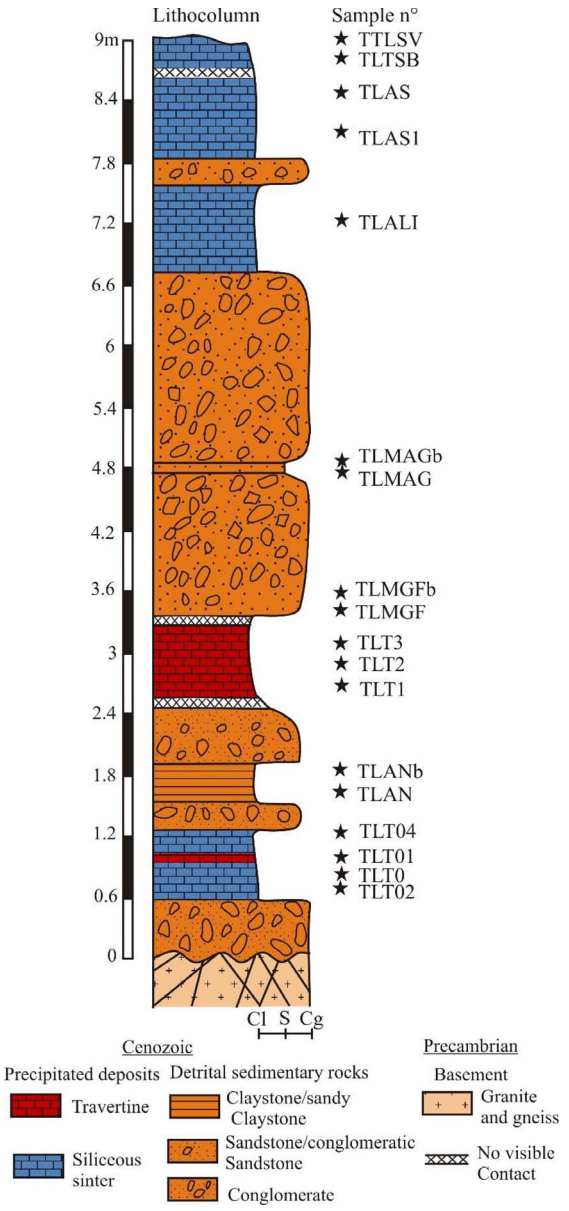

Figure 2. Synthetic litho-stratigraphic log in the study area with location of samples. Abbreviations: Cl = Clay; S = Sand; Cg = Conglomerate. Collected sample names: TLT02, TLT0, TLT01, TLT04, TLT1, TLT2, TLT3, TLALI, TLAS, TLAS1, TLTSB, TLTSV (Chemical samples) and TLAN, TLANb, TLMGF, TLMGFb, TLMGA, TLMGAb (Detrital samples).

laterally before exiting in distal outflow zones [Giggenbach et al., 1994, Handley et al., 2005, Schinteie et al., 2007, Hamilton et al., 2018, 2019]. Thermogenic travertines may therefore have been deposited from the hot spring surface distal from epithermal up-flows [Renaut and Jones, 2011].

The microtextures of hot spring precipitated deposits are much diversified and record the conditions of precipitation [e.g., Della Porta et al., 2017a, Tchouatcha et al., 2018, Hamilton et al., 2019]. They are widely described in the literature: for the travertine deposits; e.g., Kele et al. [2011] (branching or layered textures), Kanellopoulos [2012] (shrub-like, laminated, botryoidal or spicular textures), Pola et al. [2014] (porous, laminated or feather-like laminated textures), Gandin and Capezzuoli [2008] (dendritic, fibrous or plume-like textures), Della Porta [2015], Croci et al. [2016], Della Porta et al. [2017a,b] (tabular, clotted peloidal, prismatic, dendritic, fibrous, porous or columnar textures) and sinter deposits, e.g. Hamilton et al. [2019] (acicular needle-like growths, laminated, crenulated concentric, layered feathering or varved textures).

The textural characteristics (e.g., massive crystalline, vugular or coated textures) of hydrothermal deposits depend on fluid composition and CO_2 concentration [e.g., Folk et al., 1985, Pentecost, 2005, Tchouatcha et al., 2018]. For example, they display a diagenetic continuum of the silica phase from amorphous silica to hexagonal microcrystalline quartz [Herdianita et al., 2000, Rodgers et al., 2004].

According to Sillitoe [1993] and Guido and Campbell [2011], sinter deposits occur at the intersection of water table and Earth's surface, in subaerial volcanic fields where heat input is sufficient to move hydrothermal flow of ground water from deep-seated reservoirs.

The world geography of mineralized hot springs is largely dominated by travertine facies. Although travertine-siliceous sinter coexistence is rare, it is however reported in the Yellowstone National Park, USA [Fouke et al., 2000, Braunstein and Lowe, 2001, Chafetz and Guidry, 2003, Lowe and Braunstein, 2003, Hinman and Walter, 2005] and at southern Lake Bogoria, Kenya [Renaut et al., 2017].

In this study, the geochemical (major and trace elements, stable carbon and oxygen isotopes) and mineralogical (XRD and heavy minerals) analyses of varied hydrothermal deposits are presented, with the

aim to constrain the origin of fluids and dissolved elements for the hydrothermal deposits in the Laopanga area, and their conditions of deposition and chemical variations. A correlation with other CVL hot spring deposits will be established.

2. Geological setting

The CVL (Figure 1A), on which is located the study area, is a volcanic megastructure [Benkhelil, 1982, Fitton, 1983] comparable to the Benue trough [Fitton, 1983, Dunlop, 1983]. Its origin is attributed to the rejuvenation of the Central Cameroon Shear Zone (CCSZ) and Precambrian faults [Burke et al., 1971, Ngangom, 1983, Browne and Fairhead, 1983, Tchouatcha, 2011]. From Niger-Nigeria to Cameroon, the interaction between the Precambrian faults and hot spots controlled the magmatic expression during the Phanerozoic times [Ngako et al., 2006]. Precambrian tectonic rejuvenation during Phanerozoic times are well documented [Le Maréchal and Vincent, 1971, Ngangom, 1983, Dumont, 1984, 1987, Njike Ngaha, 1984, Tchouatcha et al., 2010, 2016, 2018]. They induced the Cenozoic thermo-metamorphism [Ngangom, 1983] that affected the basal Cretaceous conglomerates along the CCSZ in Djerem-Mbere [Tchouatcha, 2011, Tchouatcha et al., 2016] and are also related to the South Atlantic Ocean opening. In this particular context, the CVL represents a N30E megasplit stress related to the Pan African N70E leap reactivation [Cornacchia and Dars, 1983, Moreau et al., 1987, 1994, Deruelle et al., 1991, Montigny et al., 2004].

The study area is located on the Adamawa Plateau near the Ngaoundere region (Figure 1B), and varied basement and volcanic rocks, consisting of pre-Pan African granitoids and metamorphic formations are exposed in this area [Tchameni et al., 2006], Figure 1D). The granitoids are intensively deformed and metamorphosed under the amphibolite-facies. Monazite dating is not conclusive, but strongly indicates pre-magmatic monazite inheritance at ca. 926 Ma [Tchameni et al., 2006]. The volcanic rocks composed of mafic lava flows (basanites, alkali basalts and hawaiites) dated at 7.8 ± 1.4 Ma to 6.5 ± 0.2 Ma are associated with abundant phonolite and trachyte domes and plugs dated from 10.9 ± 0.4 Ma to 6.2 ± 0.2 Ma [Marzoli et al., 1999, Temdjim et al., 2004].

Our field work at Laopanga shows that the sedimentary basin is crossed by hot spring (40 °C) which lead to the formation chemical precipitates (travertines and siliceous sinters) alternating with detrital deposits containing varied volcanic debris (conglomerates, sandstones and claystones) from continental erosion, indicating the post-volcanic deposits, probably the Plio-Pleistocene to Actual age, according to the geochronological data of volcanic rocks [Marzoli et al., 1999, Temdjim et al., 2004]. Intense fracturing and shearing affecting the granitic basement overlain in unconformity by these deposits, indicate the important role of tectonics control on the deep fluids and their circulation. The other hot springs, with only travertine deposits, are known along the CVL such as at Ngol (29 °C) near Mount Manengouba with a cascade morphology and Bongongo (49 °C) near Mount Cameroon in a swampy area [Bisse et al., 2018, Tchouatcha et al., 2018].

3. Methods

The study area is located in a mall depression (<0.15 Km length) near Laopanga village. Twenty-five representative samples of various rock types (detrital and chemical facies) were collected on an 8 to 10 m stratigraphic spacing, were subjected to petrography, geochemistry (major and trace elements, REE and carbon and oxygen isotopes) and mineralogy (XRD and heavy minerals).

Twenty polished thin sections (sandstone, claystone, travertine, calcareo-siliceous sinter and sinter) were prepared at Langfang Rock Detection Technology Services Ltd in Hebei (China). Their microscopic study was carried out using a polarized microscope at the Laboratory of Petrology and Structural Geology of the University of Yaoundé 1 in Cameroon.

X-ray diffraction patterns were obtained from a Bruker D8-Avance Eco 1 Kw diffractometer (Copper $K\alpha$ radiance, $\lambda = 1.5418$ Å, $V = 40,125$ KV, $I = 25$ Ma) with Lynxeye Xe energy dispersive detector in the laboratory of "Argiles, Géochimie et Environnements Sédimentaires (AGES)" at the University of Liège in Belgium. The analyses were carried out on the non-oriented powder with grinded particles <50 μm of bulk material of eleven (11) representative chemical samples (travertine, calcareo-siliceous sinter and sinter).

Geochemical analyses of eighteen whole rock samples were carried out at Bureau Veritas Commodities, Vancouver, Canada. Prepared samples (homogenized powder) were mixed with LiBO2/Li2B4O7 flux. Crucibles were fused in a furnace at 1000 °C. The cooled bead was dissolved in ACS grade nitric acid. Trace elements (including rare earth elements = REE) were determined by the inductively coupled plasma mass spectrometry (ICP-MS). Major elements oxides were obtained by inductively coupled plasma-atomic emission spectrometry (ICP-AES). Loss on ignition (LOI) was determined by igniting a sample split then measuring the weight loss. The assays uncertainties varied from 0.1% to 0.04% for major elements, 0.1 to 0.5% for trace elements and 0.01 to 0.5 ppm for rare earth elements. Accuracy for REE is estimated at 5% for concentrations >10 ppm and 10% when lower. The analyzed samples concern twelve (12) pure chemical samples (travertine, calcareo-siliceous sinter and sinter) and six (06) detrital samples with chemical binder (claystone and sandstone).

Chemical deposits from study area are highly dominated by siliceous facies. The carbonate beds differ from sinter beds in colour and structure, and contained enough carbonates to be analyzed for stable isotopes. Nine samples (09) from carbonate beds (<1 m-thick for the total) were used for stable isotope analyses. They were micro-drilled from cut surfaces corresponding to areas subjected to thin section study. Analyses were performed at the University of Erlangen (Germany). Samples were reacted with 100% phosphoric acid [density > 1.9; Wachter and Hayes, 1985] at 75 °C using a Kiel III online carbonate preparation line connected to a Thermo-Finnigan 252 mass spectrometer. All values are reported in per thousand (‰) relative to V-PDB. Reproducibility was checked by replicate analysis of laboratory standards and was better than ±0.04‰ (for $\delta^{13}C$) and 0.07‰ ($\delta^{18}O$).

The method for heavy minerals analysis is that of Parfenoff et al. [1970]. After crushing (detrital deposits: sandstone and conglomerate matrix) and decalcification by HCl (travertine deposits), the heavy minerals ($d > 2.89$) of six (06) samples were extracted using "bromoform" (heavy liquid). Their identification and proportions were carried out using a polarized microscope at the Laboratory of Petrology and Structural Geology of the University of Yaoundé 1 in Cameroon.

4. Results

4.1. *Field results and facies description*

The studied outcrops, located in a vegetated river valley (Figure 1C), extend over 50 m and has a height varying from 8 to 10 m. From bottom to top, the succession consists of an alternation of precipitated (travertine and sinter) and detrital (claystone, sandstone and conglomerate) facies that overlain the sheared and fractured granitic basement (Figure 2), the contacts between these lithologies are well visibles but sometimes buried. Their thicknesses vary from 50 cm to 4 m and 20 cm to 1.5 m respectively.

4.1.1. *Precipitated deposits*

They are represented by three lithofacies based on $CaCO_3$ and SiO_2 concentrations. They are as follows:

- **Siliceous sinter lithofacies** with $SiO_2 > 90\%$ (between 90.2 and 94.8%), $CaCO_3 < 3\%$ (between 0.14 and 2.7%);
- **Calcareous–siliceous sinter lithofacies** with $SiO_2 > 50\%$ (between 63–67%), $CaCO_3 < 50\%$ (between 28.59 and 29.91%);
- **Travertine lithofacies** with $CaCO_3 > 50\%$ (between 54 and 83%), $SiO_2 < 40\%$ (between 9.1 and 39.1%).

The main characteristics of the deposits of each of the three groups are as follows:

Calcareo-siliceous sinter deposits. The deposit is located near the actual hot spring with thickness <25 cm and stacked leafs (Supplementary Figure 1). They are whitish grey to yellowish grey, laminated with abundant bioclasts (plant debris fossils), compact and less porous than the previous deposits, sometimes showing varied and vertical composition or lithology (calcareous siliceous sandstones and mudstones). They are very rich in well preserved gastropods and leafs of varied shapes. Under the microscope, they show various microstructures such as clastic (Supplementary Figure 1) or bioclastic (Supplementary Figure 1) microstructures, with rare angular and infra-millimetric quartz grains and pores. Bioclasts are mainly represented by plant debris (cuticles, tissues, tiny leaves). The laminae are thin (millimeter to infra-millimeter), sigmoid or horizontal. The pores have variable sizes and shapes

(millimeter to pluri-millimeter, elongated and subspherical). Ooids are very rare.

Travertine deposits. The travertine thickness range from about 1 to 120 cm. Their surface generally bears dissolution marks (Supplementary Figure 1), with sometimes botryoidal fabric made of calcite crystals. Their color is grey-yellowish and they are either compact or wavy laminated and porous. Under the microscope, the facies is laminar with rare oolites (<0.2 mm in diameter) and abundant bioclasts (cuticles, tissues and small-sized leaves, sometimes >2 mm size) in a porous matrix. The pores are plentiful, sometimes >50%, and vary in size and shape. The laminae are horizontal or wavy. Quartz grains are rare. The laminar fabric is highlighted by oriented calcite grains. The main diagnostic features of the travertine microfacies are the branching sparitic (Supplementary Figure 1), crystalline sparitic (Supplementary Figure 1) and sometimes fibrous sparitic crystals.

Siliceous sinter deposits. The siliceous sinter deposits is the dominant precipitated deposits with 80 to 150 cm thick. Their colors vary from greyish to black. They are distorted laminated with elongate voids (Supplementary Figure 1), displaying erosional horizontal or vertical contacts with the detrital facies (conglomerates), thin and irregular laminated, rough bedded affected by vertical thin mud cracks with calcite filling (Supplementary Figure 1), showing sometimes variation between compact and porous aspects and vertical color variation linked to varied chemical composition. Under the microscope, they are laminar with ooids (<2 mm in size), bioclasts mixed with detrital grains (quartz grains mainly). Siliceous laminae are infra-millimetric and of variable shapes with wavy fabrics, anastomosed and folded, horizontal and sometimes exhibit radial structure with syntaxial needles (Supplementary Figure 1). Spherical to sub-spherical ooids or oncoids are sometimes abundant and most often agglutinated. Bioclasts are numerous and diversified with millimetric to plurimillimetric plant debris (cuticles, tissues) and small-sized (<2 mm) gastropods and ostracods (Supplementary Figure 1). The pores can be very abundant, with variable shapes and sizes (<1 cm). Detrital grains are essentially angular quartz grains associated with highly weathered minerals.

4.1.2. *Detrital deposits*

Detrital deposits consist of three main facies (claystone, sandstone and conglomerate) enclosing terrigenous debris (metamorphic, plutonic, volcanic detritus and sometimes sinter fragments in the upper part of the sequence) and sillicicalcareous binder. As the chemical deposits, they outcrop on both sides of Mambere stream that crosses the basin (Supplementary Figure 2). The main sedimentary structures affecting these facies are the bedding (Supplementary Figure 2) and lamination (Supplementary Figure 2). They are as follows:

- **Black claystone** with about 50 cm thick, is rich in organic matter (Supplementary Figure 2) with abundant angular quartz and feldspar grains, in a very fine to fine-grained fabric (Supplementary Figure 2);
- **Pink sandstone rich** in feldspars (microcline essentially associated with plagioclase and orthoclase) and quartz associated with ferricrusts, basalts, granites, gneiss debris, siliceous/calcareous binders and sometimes clayey matrix in a fine to coarse-grained fabric (Supplementary Figure 2). The thickness range between 25 to 100 cm;
- **Pink conglomerates** with same mineralogical composition as the previous sandstones associated with pebbles of same lithology (ferricrusts, basalts, granites, gneiss) but in a medium to very coarse-grained fabric, and the thickness varying from 60 to 200 cm.

4.2. *Geochemistry*

The precipitated materials (Supplementary Tables 1, 2, and 3) were divided into two groups: (i) travertine/carbonate group (T: $CaCO_3$ > 50%), and (ii) siliceous sinter group (ST: SiO_2 > 50%). An additional detrital sedimentary rocks (DSR) is also recognized and will allow comparisons with purely chemical facies.

4.2.1. *Major elements*

Normalized to PAAS [Post Archean Australian Shale, McLennan, 2001] (Figure 3), ST samples are, as expected, more enriched in SiO_2 which is depleted in the T group. ST and T samples are enriched in CaO, mainly in the T group, and depleted in the

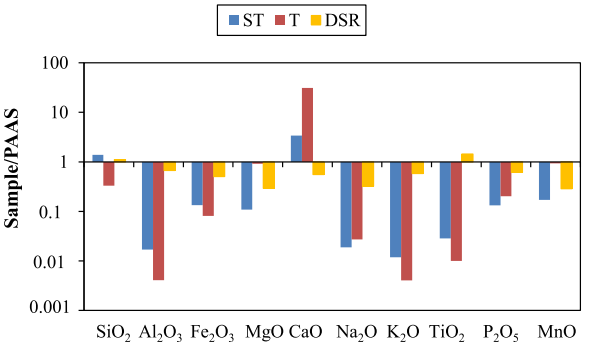

Figure 3. Stick diagram of average major elements normalized to PAAS [McLennan, 2001] Abreviations: ST = siliceous sinter and calcareo-siliceous sinter; T = travertine; DSR = detrital sedimentary rock.

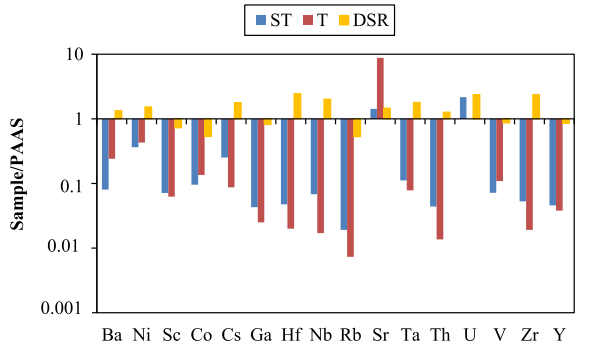

Figure 4. Stick diagram of average trace elements normalized to PAAS [McLennan, 2001]. Abreviations: ST = siliceous sinter and calcareo-siliceous sinter; T = travertine; DSR = detrital sedimentary rock.

DSR group. This latter is enriched in TiO_2 which is depleted in the two other groups. The three groups (T, ST, and DSR) are depleted in all the remaining elements (Al_2O_3, Fe_2O_3, MgO, Na_2O, K_2O, P_2O_5 and MnO).

4.2.2. *Trace elements*

Normalized to the PAAS [McLennan, 2001] the T samples are more enriched in Sr, and ST and DSR samples are enriched in U (Figure 4). The main remaining elements (Ba, Ni, Cs, Hf, Nb, Ta, Th and Zr) are depleted in the precipitated facies and enriched in the detrital ones, except for Sc, Co, Ga, Rb, V and

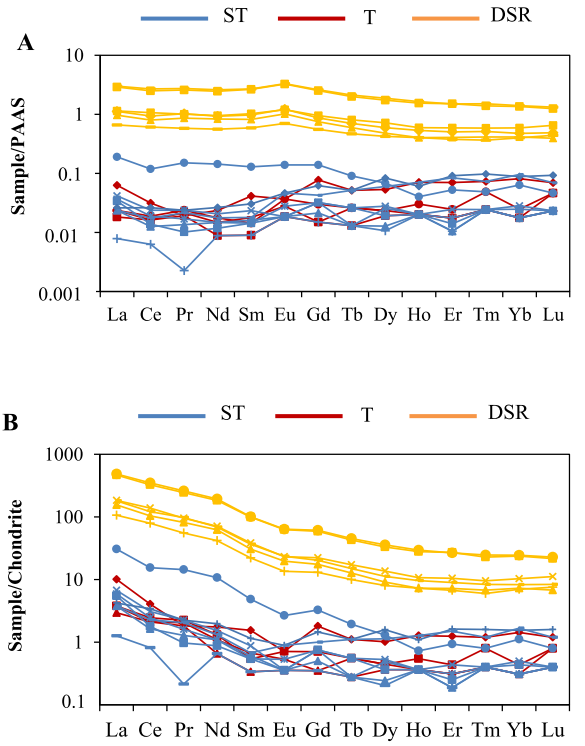

Figure 5. Distribution patterns of rare elements normalized to PAAS (A) and Chondrite (B) after McLennan [2001] and McDonough and Sun [1995] respectively.

Y depleted. Th contents vary from 3.2 to <0.2 ppm in the precipitated deposits and from 9.4 and 31.1 ppm in the detrital facies, with U concentrations ranging from 1.1 to 13.3 ppm and 3 to 12.1 ppm respectively. Sr varies from 17.5 to 2304.1 ppm (17.5 to 2304.1 ppm and 184.1 to 455.9 ppm respectively in precipitated and detrital facies). The dominant elements in the studied facies are Sr, Ba and Zr.

4.2.3. *Rare earth elements*

PAAS and chrondrite-normalized [McLennan, 2001 and McDonough and Sun, 1995 respectively] REE pattern show that the precipitated deposits are more depleted in REE than the detrital deposits grouped upwards (Figure 5A and B). The precipitated sample TLALI from ST group is more enriched in high REE probably linked to a contamination from the detrital deposits. The precipitated sample TLTO from ST group shows a negative Pr anomaly. The

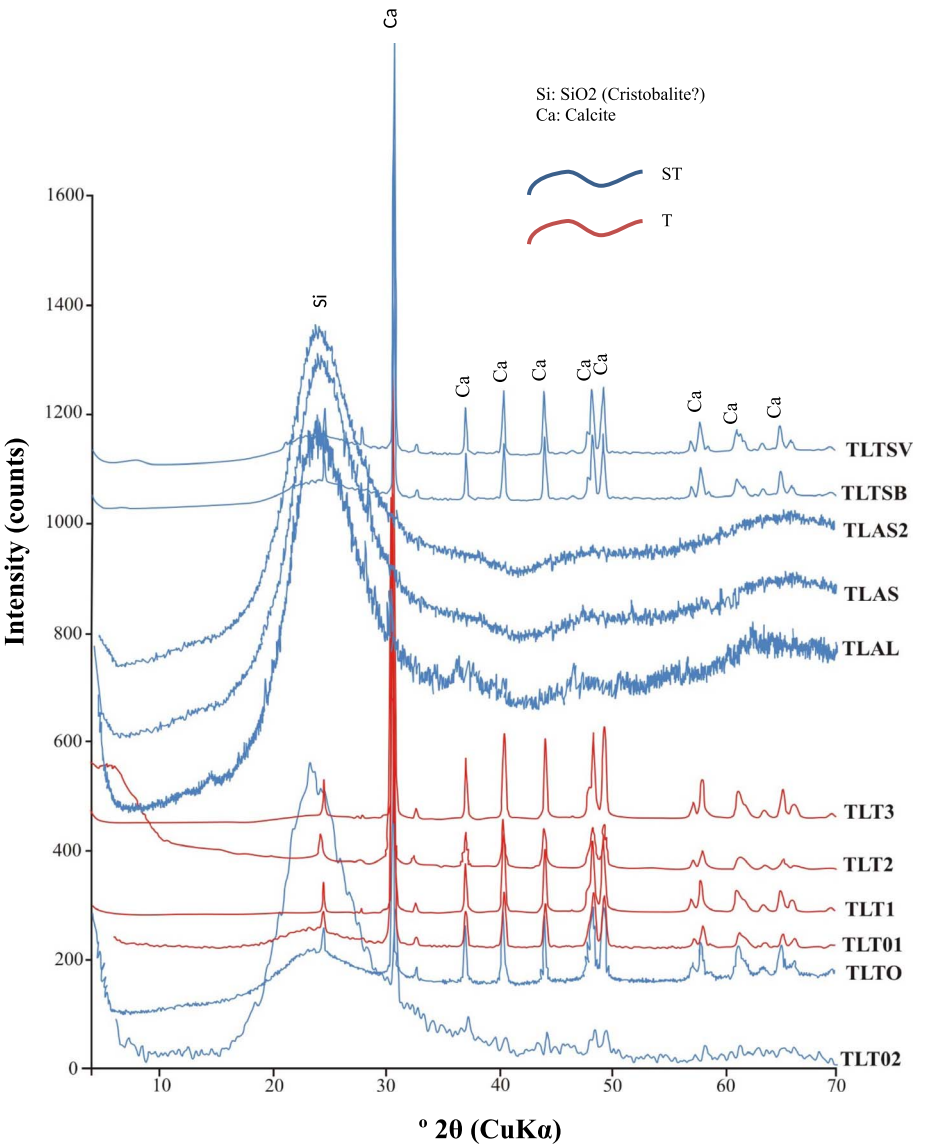

Figure 6. Vertical X-ray diffraction from the chemical deposits (see Figure 2 for stratigraphic position of the studied samples).

fine-grained sediments (TLAN and TLANb) from DSR facies are more enriched than those of coarse-grained.

4.3. *Mineralogy*

4.3.1. *X-ray diffraction (XRD)*

Amorphous silica is characterized by a diffuse peak in all samples from 10 to 30° angular limits (XRD diagrams) typical of non-crystallized silica [Biswas et al., 2018]. The strong intensity of the peaks indicates a high proportion of amorphous silica, cristobalite [Le Maréchal, 1976] in the siliceous samples from ST group) except for samples rich in calcite samples from T group (Figure 6).

In the ST group, the remaining samples (TLTO, TLTSV and TLTSB) contain calcite. The composition is strongly dominated at the base of the profile by silica (sample TLO2), then occurs a slight

silica depletion (sample TLT0), followed by an important depletion of silica and an enrichment of calcite (samples TLT01, TLT1 and TLT3). Finally, an enrichment in silica (samples TLALI and TLAS) with a slight depletion and enrichment in silica and calcite respectively (samples TLTSB and TLTSV) occur at the top of the profile.

4.3.2. *Heavy minerals*

Heavy minerals from chemical and detrital samples reveal a great diversification with kyanite, epidote, tourmaline, zircon, hornblende and oxides (Supplementary Figure 3). However, the mineral assemblages present a strong heterogeneity despite, as a general rule, oxides dominate. Meanwhile, tourmaline is rare to absent in the detrital samples and basaltic hornblende is present in the detrital samples and absent in the chemical deposits. Their grain shapes are very angular to angular.

4.4. *Stable carbon and oxygen isotopes*

Carbon and oxygen isotope compositions of nine samples are given in Supplementary Table 4. The carbon and oxygen isotope values are perceptibly similar or very close, with $\delta^{13}C$ varying from 1.54 to 2.90‰ V-PDB and $\delta^{18}O$ from −10.1 to −6‰ V-PDB or 20.50 to 24.34‰ SMOW. These values are comparable with the average carbon and oxygen isotopic compositions of hot spring deposits out and from Cameroon (Figure 7) [Della Porta et al., 2017a].

5. Discussion

5.1. *Origin of deposition*

The water origin is given by stable isotopes [Craig, 1953, Minissale et al., 2002, Kele et al., 2011, Della Porta et al., 2017a, Bisse et al., 2018, Matera et al., 2021] and the solute give idea on the fluid rock [Le Maréchal, 1976].

5.1.1. *Stable isotope and hot spring composition interpretations*

Although only nine oxygen and carbon isotopic compositions have been recorded from the studied stratigraphic column, they are representative of the series because they cluster around values that are very close to each other. Carbon isotopes are widely used to characterize the origin of travertine deposits [Craig, 1953, Turi, 1986, Cerling et al., 1991, Kele et al., 2011, Bisse et al., 2018], as their isotopic compositions are essentially controlled by $\delta^{13}C$ values of parental CO_2 sources. These values can be superficial (atmospheric and soil gas) or of deep origin; crustal metamorphism, magma/mantle degassing, ancient deep crystallized igneous melt or hydrocarbon [Ohmoto and Rye, 1979, Hoefs, 1987, Pentecost and Viles, 1994]. Pentecost and Viles [1994] have, for example, differentiated thermogenic or hydrothermal travertine from meteoric deposits or ambient temperature deposits (tufa) according to the carbon origin. These travertines are characterized by $\delta^{13}C$ values that vary from 0‰ to −11‰ while the thermogenic ones range from −4‰ to +8‰ [Turi, 1986, Pentecost, 2005, Guo and Chafetz, 2014]. According to Jones and Renaut [2010], Rodríguez-Berriguete et al. [2012] and Pentecost [2005], the positive carbon isotopic signatures are characteristic of thermogenic travertines. The $\delta^{13}C$ values from our studied samples are positive and vary from 1.54‰ to 2.90‰, very low than other values such as those from the travertine in the Central Italy [e.g., Della Porta, 2015, Della Porta et al., 2017b] indicating likely the downstream CO_2 degassing while thermal water is flowing and the low effect of dissolved substrate carbonate [e.g., Gonfiantini et al., 1968, Minissale et al., 2002, Della Porta, 2015, Della Porta et al., 2017a] that could be mainly the Precambrian magmatic and metamorphic rocks as indicate the hot water source composition [Le Maréchal, 1976]. Also, the combined plot of carbon and oxygen isotopic compositions indicates a thermogenic origin, in agreement with data of Gandin and Capezzuoli [2008], Pola et al. [2014], Della Porta et al. [2017a].

The hot spring compositions from which precipitated deposits have been used to characterize the origin of various travertines [Bisse et al., 2018, Tchouatcha et al., 2018]. Spring of the study area is warm (40 °C), highly mineralized (1680 mg/l), with slight acidity (pH = 6) and rich in dissolved CO_2 (560 mg/l) [Le Maréchal, 1976], characteristic of deep-derived endogenic water as suggested by Crossey et al. [2006]. The hot nature of this spring suggests therefore a thermogenic origin the travertines [Casanova, 1981, Magnin et al., 1991]. This quite weak temperature (40 °C) is lower than the one expected for water heated by a magma chamber and

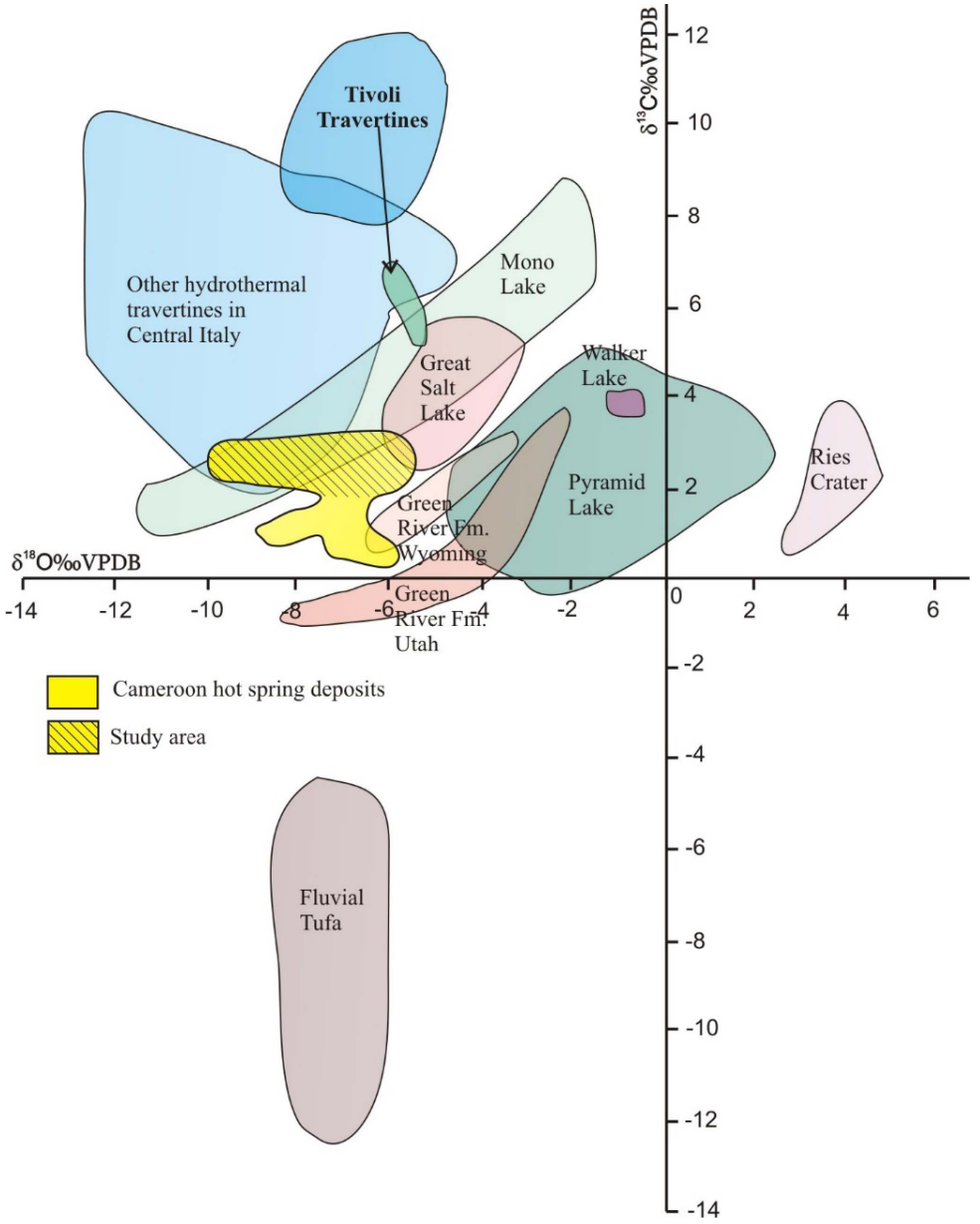

Figure 7. Combined plot of δ^{18}O‰ (PDB) δ^{13}C‰ (PDB) values from travertines presently forming in terrestrial environments [slightly modified Della Porta et al., 2017a]. The δ^{18}O and δ^{13}C of our studied samples fall in the upper part of the diagram confirming a geothermal provenance of the depositing parental water.

could be explained by the consequent heat loss during the water rising toward the subsurface. δ^{13}C values (1.54‰ to 2.90‰) point effectively to a mixture of deep and fresh waters [Crossey et al., 2006].

The presence of a thin layer of travertine in the siliceous sinter deposit can be related to late-stage fluid deposits of different composition [Drake et al., 2014, Guido and Campbell, 2017, Campbell et al., 2019], on the one hand, and on the other hand, deposition of both silica and calcite is likely controlled by microchemical conditions and local temperature gradient [Campbell et al., 2002], moreover,

the evidence of the Cyanobacteria and other bacteria role in calcite and aragonite nucleation in hot springs (40 °C for Laopanga hot spring) as the thermophilic microbes have long been implicated in the formation of travertine and siliceous sinter [e.g., Renaut and Jones, 2000, 2011, Giggenbach et al., 1994, Schinteie et al., 2007, Della Porta et al., 2022]. The vertical variation of some characteristic chemical minerals is given in Supplementary Figure 4 showing the same evolution between CaO and Sr curves from the bottom to the top, contrary to the SiO_2 evolution, and the same evolution between $\delta^{13}C$ and $\delta^{18}O$ curves from the bottom to the top.

5.1.2. *Geological hypothesis*

Main mineral/water rock genetic types in the Earth's crust related to recent volcanic and thermometamorphic activities have been described by Ivanov et al. [1968]. Their data have been applied in the Mbere sub-basin exposing travertines [Tchouatcha et al., 2016] along the active CVL [Suh et al., 2003]. Relationships between CVL and CCSZ (Central Cameroon Shear Zone) [Tchouatcha et al., 2016], and several reactivations of the Precambrian faults indicate that an intense fracturation was associated with exsurgence and resurgence phenomena in CVL related to a deep endogenic spring [Tchouatcha et al., 2018]. The weak thermosmetamorphism that affected the Cretaceous conglomerates along CCSZ indicates a Cenozoic reactivation of these faults [Ngangom, 1983, Dumont, 1987, Tchouatcha et al., 2010, 2016, Tchouatcha, 2011]. Many authors have established a link between travertines (hot spring deposits) and active tectonics [Pentecost, 1995, Tchouatcha et al., 2016, 2018]. In Cameroon, some compounds appear to be specific to the geological environment; in the hot spring, chlorine (Cl) element is generally linked to volcanic phenomena and sulphur (SO_4) to tectonic phenomena, while carbon dioxide (CO_2) appears to be ubiquitous, although its dominant activity in a volcanic environment [Le Maréchal, 1976]. These values are 1054.72 mg/l (Cl), 40.30 mg/l (SO_4) and 500 mg/l (CO_2) at Bongongo, 5.67 mg/l (Cl), 7.20 mg/l (SO_4) and 1050 mg/l (CO_2) at Ngol, and 12.40 mg/l (Cl), 41.79 mg/l (SO_4) and 560 mg/L (CO_2) at Laopanga respectively [Le Maréchal, 1976]; at Laopanga, the SO_4 value (41.79 mg/L) is high than that of Cl (12.40 mg/L) and those of Bongongo (40.30 mg/L) and Ngol (7.20 mg/L) hot springs, indicating the important role of tectonics control on Laopanga hot spring deposits, as the cases in Turkey [e.g., Altunel and Hancock, 1993, Altunel and Karabacak, 2005, Mesci et al., 2008], Italy [e.g., Brogi et al., 2012, De Filippis et al., 2013a; and Greece Kanellopoulos et al., 2017]. Moreover, the variety of hydrothermal deposits grow in the cooling geothermal system when and where outflow from distal silica-rich chloride parent fluids or deep alkali chloride parent fluids upflow are replaced by CO_2-rich fluids leads to the deposits of travertine [Renaut and Jones, 2011].

Heavy mineral distribution in the chemical deposits indicates that the deep water flowed across metamorphic (such as gneisses) and plutonic rocks (such as granites). The reported epidote is probably derived from hydrothermal alteration of plutonic rocks through which flowed the hot water. Kyanite indicates metamorphic sources while zircon, tourmaline, garnet and hornblende are from both plutonic and metamorphic sources. Meanwhile, the presence of basaltic hornblende in the detrital deposits indicates the erosion of volcanic source rocks.

Non-crystalline or amorphous silica in the chemical deposits is related to diagenetic immaturity according to Campbell et al. [2001] and Rodgers et al. [2004] and can be explained by the lack of lattice reordering and structure water preservation, with conservation of low density and abundant porosity.

5.2. *Evidence of deep hydrothermal migration and tectonic control*

The morphological types of the studied deposits are not easy to recognize. Field observation indicates a concatenation of chemical and detrital deposits. The main preserved outcrops of chemical deposits are related to intense erosion giving sometimes galleries and one main stream crossing the deposits.

The Sr, $\delta^{18}O$ and $\delta^{13}C$ values have used to depict the origin of chemical deposits [e.g., Kele et al., 2011, Bisse et al., 2018]. In this study, the Sr concentrations values range from 17.5 to 2304.1 ppm suggest a deposition far (low values of Sr) and close (high values of Sr) to paleosprings [Kele et al., 2011]. The Sr values indicate that the travertine deposits for Bongongo and Ngol areas are respectively close and far from the paleosprings [Bisse et al., 2018]. Meanwhile, Sr values

generally increase or decrease following SiO_2 values (See Supplementary Figure 4), low in high siliceous deposits and high in low siliceous deposits, suggesting that the silica enrichment could be derived from chemical alteration of saturated bedrock with silica during distal hot water flows.

Moreover, the $\delta^{13}C$ values (varying from 1.5 to 2.9‰ V-PDB), the fabrics (bedding, lamination, ...) or some characteristic microstructures (shrubs, ...) indicate that the study chemical deposit were mainly precipitated directly from hot water.

Meanwhile, some deposits with high porosity, compact structure and with snail's preservation could indicate the periodic precipitations from cooled thermal water [Capezzuoli et al., 2014].

Positive Eu anomalies are the signatures of the hydrothermal fluids [Bau et al., 1996]. The PAAS-normalized patterns of the studied precipitated deposits display negative and positive Eu anomalies, but mainly >1 (Eu/Eu*: 0.54–1.78). These values range from 0.54 to 1.78 in the travertine facies and 0.67 to 1.66 in the siliceous to calcareous siliceous facies indicating the temperature variation of precipitation related to the distance of the deep hot water circulation. Moreover, these values are >1 and range from 1.21 to 1.27 in the detrital deposits suggesting likely the thermogenic effect from precipitated deposits as they constitute the matrix of these facies.

Furthermore, the black claystones associated with the laminations and bedding that affected the basal conglomerates point to more reduced environment created by tectonics. The presence towards the upper part of the sequence of a distorted bed of siliceous sinter suggests a filling up period. So, sedimentation and precipitation took place in an active paleotectonic basin (Figure 8). Evidence of the reactivation of old faults is reported both on the basement and ancient sedimentary deposits of the Cretaceous age [Ngangom, 1983, Dumont, 1987, Tchouatcha, 2011].

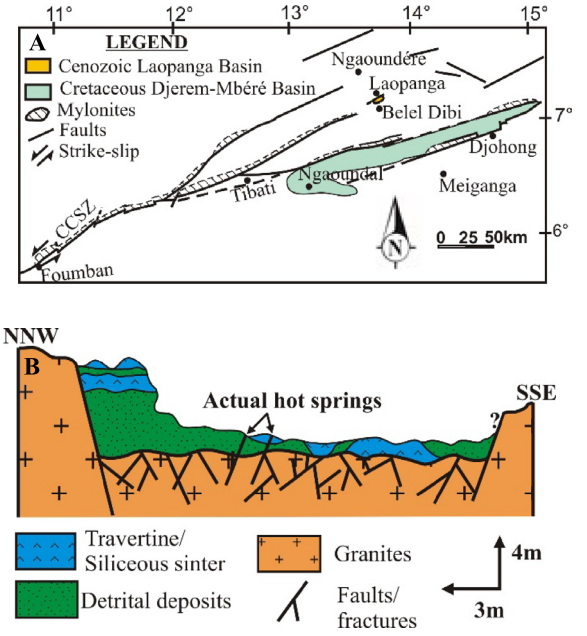

Figure 8. (A) Location of the Laopanga Basin in a faulted corridor [modified from Le Maréchal, 1976] and evidence of relationship with the Precambrian faults (CCSZ) reactivation. (B) Schematic geological sketch and interpretative depositional model between detrital and chemical deposits and showing intense fault networks affecting the Precambrian basement and recent deposits indicating the Post-Precambrian or Recent faults reactivation.

5.3. *Age of deposition*

The Laopanga Basin is located in the volcanic zone of the Ngaoundere area. The basal detrital deposits of this basin contains the volcanic rock debris as indicated above (heavy minerals data). The presence of siliceous and carbonated cements in this basal deposits, on the one hand, and on the other hand, the vertical contact between the basal detrital and chemical deposits, suggests approximately the same age of deposition for these deposits. Moreover, the basal deposit of the Laopanga Basin is discordant on granite affected by a N60°E trending fault similar to the CCSZ and these two faults are believed to be contemporaneous.

In the Ngaoundere area, mafic lava flows (basanites, alkaline basalts and hawaiites) are dated at 7.8 ± 1.4 to 6.5 ± 0.2 Ma, with abundant trachyte and phonolites domes and plugs emplaced at 10.9 ± 0.4 to 6.2 ± 0.2 Ma [Marzoli et al., 1999, Temdjim et al., 2004] indicating a Mio–Pliocene volcanic activities in this area. The age inferred from the palynological data as well as on the detrital deposits [Plio-Pleistocene, Tchouatcha et al., 2010] and that of travertine deposits [Pleistocene Holocene, Tchouatcha et al., 2016] in the Mbere Basin located

along the CCSZ, and the ages of volcanic rocks in the studied area [Marzoli et al., 1999, Temdjim et al., 2004] suggest a Plio-Pleistocene to Actual age for the Laopanga hot spring deposits.

6. Conclusion

- According to the major elements chemical composition, and the Sr concentrations, the hot spring deposits of Laopanga vary from travertines to siliceous sinters, and are likely related to the upflow and outflow of parental fluids, and The Eu/Eu* values indicate the temperature variation of precipitated deposits related to distance of the deep hot water flow;
- $\delta^{13}C$ and $\delta^{18}O$ isotope values of carbonates fall in the values typical of a thermogenic source for the deposits, although they are very far from the isotopic composition of magmatic carbon, because there is isotopic fractionation during water rising. The carbon isotope value (>0‰) suggests that the deposits are from deep and hot waters rich in CO_2;
- The location of the study area in a volcanic zone belonging to the Cameroon volcanic line, the relationship between the Cameroon volcanic line and the Central Cameroon Shear Zone, and the intense fracturing and shearing affecting the granitic basement indicate the important role of tectonics control on the Laopanga deposits;
- The variation between the siliceous sinter and travertine, indicate likely intense geothermal up-flow and outflow along the CVL, and the age of Laopanga deposits ranges from Plio-Pleistocene to Actual according to the volcanic rocks age in the studied area and the relationship between these volcanic rocks and deposits.

Declaration of interests

The authors do not work for, advise, own shares in, or receive funds from any organization that could benefit from this article, and have declared no affiliations other than their research organizations.

Acknowledgements

We thank Professors Giovanna Della Porta and Stanislas Sizaret, and the Editor for their for their constructive comments to improve the quality of this work.

Supplementary data

Supporting information for this article is available on the journal's website under https://doi.org/10.5802/crgeos.230 or from the author.

References

Altunel, E. and Hancock, P. (1993). Active fissuring and faulting in quaternary travertines at pamukkale, Western Turkey. In Stewart, I. S., Vita-Finzi, C., and Owen, L. A., editors, *Neotectonics and Active Faulting: Zeitschrift fuer Geomorphologie Supplement*, volume 94, pages 285–302.

Altunel, E. and Karabacak, V. (2005). Determination of horizontal extension from fissure ridge travertines: a case study from the Denizli Basin, Southwestern Turkey. *Geodinam. Acta*, 18, 333–342.

Bau, M., Koschinsky, A., Dulski, P., and Hein, J. R. (1996). Comparison of the partitioning behaviours of yttrium, rare earth elements, and titanium between hydrogenetic marine ferromanganese crusts and seawater. *Geochim. Cosmochim. Acta*, 60, 1709–1725.

Benkhelil, J. (1982). Benue trough and benue chain. *Geol. Mag.*, 119(2), 155–168.

Berardi, G., Vignaroli, G., Billi, A., Rossetti, F., Soligo, M., Kele, S., Baykara, M. O., Bernasconi, M. S., Castorina, F., Tecce, F., and Shen, C. C. (2016). Growth of a Pleistocene giant carbonate vein and nearby thermogene travertine deposits at Semproniano, southern Tuscany, Italy: estimate of CO_2 leakage. *Tectonophysics*, 690, 219–239.

Bisse, S. B., Ekomane, E., Eyong Takem, J., Ollivier, V., Douville, E., Maffo Nganne, M. J., Bokanda Ekoko, E. L., and Bitom, D. (2018). Sedimentological and geochemical study of the Bongongo and Ngol travertines located at the Cameroon volcanic line. *J. Afr. Earth Sci.*, 143, 201–214.

Biswas, R. K., Khan, P., Mukherjee, S., Mukhopadhyay, A. K., Ghosh, J., and Muraleedharan, K. (2018).

Study of short range structure of amorphous silica from PDF using Ag radiation in laboratory XRD system, RAMAN and NEXAFS. *J. Non-Cryst. Solids*, 488, 1–9.

Braunstein, D. and Lowe, R. L. (2001). Relationship between spring and geyser activity and the deposition and morphology of high temperature (>73 °C) siliceous sinter, Yellowstone National Park, Wyoming, USA. *J. Sediment. Res.*, 71(5), 747–763.

Brogi, A., Alçiçek, M. C., Liotta, D., Capezzuoli, E., Zucchi, M., and Matera, P. F. (2021a). Step-over fault zones controlling geothermal fluid-flow and travertine formation (Denizli Basin, Turkey). *Geothermics*, 89, article no. 101941.

Brogi, A., Capezzuoli, E., Buracchi, E., and Branca, M. (2012). Tectonic control on travertine and calcareous tufa deposition in a low-temperature geothermal system (Sarteano, Central Italy). *J. Geol. Soc.*, 169, 461–476.

Brogi, A., Capezzuoli, E., Karabacak, V., Alcicek, M. C., and Luo, L. (2021b). Fissure ridges: A reappraisal of faulting and travertine deposition (Travitonics). *Geosciences*, 11, article no. 278.

Brogi, A., Liotta, D., Capezzuoli, E., Matera, P. L., Kele, S., Soligo, M., Tuccimei, P., Ruggieri, G., Yu, T., Shen, C. C., and Huntington, K. W. (2020). Travertine deposits constraining transfer zone neotectonics in geothermal areas: An example from the inner Northern Apennines (Bagno Vignoni-Val d'Orcia area, Italy). *Geothermics*, 85, article no. 101763.

Browne, S. E. and Fairhead, J. D. (1983). Gravity study of the Central African rift system: a model of continental disruption 1. The Ngaoundere and Abu Gabra rifts. *Tectonophysics*, 94, 187–203.

Burke, K. C., Dessauvagie, T. F. J., and Whiteman, A. J. (1971). Opening of the Gulf of Guinea and geological history of the Benue depression and Niger delta. *Nat. Phys. Sci.*, 223, 51–55.

Campbell, K. A., Guido, D. M., Vikre, P. G., John, D. A., Rhys, D., and Hamilton, A. R. (2019). The Miocene Atastra Creek sinter (Bodie Hills volcanic field, California and Nevada): 4D evolution of a geomorpologically intact siliceous hot–spring deposit. *J. Volcanol. Geotherm. Res.*, 370, 65–81.

Campbell, K. A., Rodgers, K. A., Brotheridge, J., and Browne, P. R. L. (2002). An unusual modern silica–carbonate sinter from Pavlova spring, Ngatamariki, New Zealand. *Sedimentology*, 49(4), 835–854.

Campbell, K. A., Sannazzaro, K., Rodgers, K. A., Herdianita, N. R., and Browne, P. R. L. (2001). Sedimentary facies and mineralogy of the Late Pleistocene Umukuri silica sinter, Taupo Volcanic Zone, New Zealand. *J. Sediment. Res.*, 71(5), 727–746.

Capezzuoli, E., Gandin, A., and Pedley, M. (2014). Decoding tufa and travertine (fresh water carbonates) in the sedimentary record: The state of the art. *Sedimentol*, 61, 1–21.

Casanova, J. (1981). *Morphologie et biolithogenèse des barrages de travertin, formations carbonatees externes, tufs et travertins*, volume 3. Edition du Comité National de Geographie Française, in Mémoire de l'Association Française de Karstologie.

Cerling, T. E., Solomon, D. K., Quade, J., and Bowman, J. R. (1991). On the isotopic composition of carbon in soil carbon dioxide. *Geochim. Cosmochim. Acta*, 55, 3403–3406.

Chafetz, H. S. and Guidry, S. A. (2003). Deposition and diagenesis of Mammoth hot springs travertine, Yellowstone National Park, Wyoming, USA. *Can. J. Earth Sci.*, 40(11), 1515–1529.

Cornacchia, M. and Dars, R. (1983). Un trait structural majeur du continent africain. Les linéaments centrafricains du Cameroun au Golfe d'Aden. *Bull. Soc. Géol.*, 1, 101–109.

Craig, H. (1953). The geochemistry of stable carbon isotope. *Geochim. Cosmochim. Acta*, 3, 53–92.

Croci, A., Della Porta, G., and Capezzuoli, E. (2016). Depositional architecture of a mixed travertine-terrigenous system in a fault-controlled continental extensional basin (Messinian, Southern Tuscany, Central Italy). *Sediment. Geol.*, 332, 13–39.

Crossey, L. J., Fischer, T. P., Patchett, P. J., Karlstrom, K. E., Hilton, D. R., Newell, D. L., Huntoon, P., Reynolds, A. C., and De Leeuw, G. A. M. (2006). Dissected hydrologic system at the Grand Canyon: interaction between deeply derived fluids and plateau aquifer water in modern springs and travertine. *Geol. Soc. Am.*, 34, 25–28.

De Filippis, L., Anzalone, E., Billi, A., Faccenna, C., Poncia, P. P., and Sella, P. (2013a). The origin and growth of recently ridge travertine over a seismic fault, Tivoli, Italy. *Geomorpholgy*, 195, 13–26.

De Filippis, L., Faccenna, C., Billi, A., Anzalone, E., Brilli, M., Soligo, M., and Tuccimei, P. (2013b). Plateau versus fissure ridge travertines from Quaternary geothermal spring of Italy and Turkey: in-

teractions and feedbacks between fluid discharge, paleoclimate, and tectonics. *Earth Sci. Rev.*, 123, 35–52.

Della Porta, G. (2015). Carbonate build-ups in lacustrine, hydrothermal and fluvial settings: comparing depositional geometry, fabric types and geochemical signature. In Bosence, D. W. J., Gibbons, K. A., Le Heron, D. P., Morgan, W. A., Pritchard, T., and Vining, B. A., editors, *Microbial Carbonates in Space and Time: Implication for Global Exploration and Production*, Geological Society, London, Special Publications 418, pages 17–68. Geological Society of London.

Della Porta, G., Capezzuoli, E., and De Bernado, A. (2017a). Facies character and depositional architecture of hydrothermal travertine slope aprons (Pleistocene, Acquasanta Terme, Central Italy). *Mar. Petrol. Geol.*, 87, 171–187.

Della Porta, G., Croci, A., Marini, M., and Kele, S. (2017b). Depositional architecture, facies character and geochemical signature of the Tivoli travertines (Pleistocene, Acque Albule Basin, Central Italy). *Rev. Ital. Paleontol. Stratigr.*, 123(3), 487–540.

Della Porta, G., Hoppert, M., Hallmann, C., Schneider, D., and Reitner, J. (2022). The influence of microbial mats on travertine precipitation in active hydrothermal systems (Central Italy). *Depositional Rec.*, 8(1), 165–209.

Deruelle, B., Moreau, C., Nkoumbou, C., Kambou, R., Lissom, J., Njongfang, E., Ghogomu, R. T., and Nono, A. (1991). The Cameroon Line: a review. In Kampunzu, A. B. and Lubala, R. T., editors, *Magmatism in Extentional Structural Settings. The Phanerozoic Africa Plate*, pages 274–327. Springer, Berlin.

Drake, B. D., Campbell, K. A., Rowland, J. V., Guido, D. M., Browne, P. R. L., and Rae, A. (2014). Evolution of a dynamic paleo–hydrothermal system at Mangatete, Taupo Volcanic Zone, New Zealand. *J. Volcanol. Geother. Res.*, 282, 19–35.

Dumont, J. F. (1984). *Etude structurale de l'Adamaoua et de sa marge Nord*. Cahiers ORSTOM-IRGM, Cameroun.

Dumont, J. F. (1987). Etude structurale des bordures nord et sud du plateau de l'Adamaoua: influence du contexte atlantique. *Géodynamique*, 2(1), 55–68.

Dunlop, H. M. (1983). *Strontium Isotope Geochemistry and Potassium-Argon Studies on Volcanic Rocks from the Cameroon Line, West Africa*. PhD thesis, University of Edinburgh.

Faccenna, C., Soligo, M., Billi, A., De Filippis, L., Funiciello, R., Rossetti, C., and Tuccimei, P. (2008). Late Pleistocene depositional cycles of *Lapis tiburtinus* travertine (Tivoli, Central Italy): possible influence of climate and fault activity. *Glob. Planet. Change*, 63, 299–308.

Fitton, J. G. (1983). Active versus passive continental rifting: evidence from the West African rift system. *Tectonophysics*, 94, 473–481.

Folk, R. L., Chafetz, H. S., and Tiezzi, P. A. (1985). Bizarre forms of depositional and diagenetic calcite in hot-spring travertines, Central Italy. *SEPM Spec. Publ.*, 36, 349–369.

Fouke, B. W., Farmer, J. D., Des Marais, D. J., Pratt, L., Sturchio, N. C., Burns, P. C., and Discipulo, M. K. (2000). Depositional facies and aqueous–solid geochemistry of travertine depositing hot Springs (Angel Terrace, Mammoth Hot Springs, Yellowstone National Park, U.S.A.). *J. Sediment. Res.*, 70(3), 565–585.

Gandin, A. and Capezzuoli, E. (2008). Travertine versus Calcareous tufa: distinctive petrologic features and related stable isotope signatures. Il Quaternario Ital. *J. Quat. Sci.*, 21, 125–136.

Giggenbach, W., Sheppard, D. S., Robinson, B. W., Stewart, M. K., and Lyon, G. L. (1994). Geochemical structure and position of the Waiotapu geothermal field, New Zealand. *Geothermics*, 23(5), 599–644.

Giustini, F., Brilli, M., and Mancini, M. (2017). Geochemical study of travertines along middle-lower Tiber valley (Central Italy): genesis, palaeoenvironmental and tectonic implications. *Int. J. Earth Sci.*, 107, 1321–1342.

Gonfiantini, R., Panichi, C., and Tongiorgi, E. (1968). Isotopic disequilibrium in travertine deposition. *Earth Planet. Sci. Lett.*, 5, 55–58.

Guido, D. M. and Campbell, K. A. (2011). Jurassic hot spring deposits of the Deseado Massif (Patagonia, Argentina): characteristics and controls on regional distribution. *J. Volcanol. Geotherm. Res.*, 203(1–2), 35–47.

Guido, D. M. and Campbell, K. A. (2017). Upper Jurassic travertine at El Macanudo, Argentine Patagonia: a fossil geothermal field modified by hydrothermal silicification and acid overprinting. *Geol. Mag.*, 155(6), 1394–1412.

Guo, X. and Chafetz, H. S. (2014). Trends in δ^{18}O and δ^{13}C values in lacustrine tufa mounds: Palaeohydrology of Searles Lake, California. *Sedimentology*, 61, 221–237.

Hamilton, A. R., Campbell, K. A., and Guido, D. M. (2019). Atlas of siliceous hot spring deposits (sinter) and other silicified surface manifestations in epithermal environments. Lower Hutt (NZ): GNS Science Report.

Hamilton, A. R., Campbell, K. A., Rowland, J. V., Barker, S., and Guido, D. (2018). Characteristics and variations of sinters in the Coromandel Volcanic Zone: application to epithermal exploration. New Zealand. *J. Geol. Geophy.*, 62, 531–549.

Handley, K., Campbell, K. A., Mountain, B. W., and Browne, P. R. L. (2005). Abiotic–biotic controls on the origin and development of spicular sinter: in situ growth experiments, Champagne Pool, Waiotapu, New Zealand. *Geobiology*, 3(2), 93–114.

Henchiri, M., Ahmed, W. B., Brogi, A., Alçiçek, M. C., and Benassi, R. (2017). Evolution of Pleistocene travertine depositional system from terraced slope to fissure-ridge in a mixed travertine-alluvial succession (Jebel El Mida, Gafsa, southern Tunisia). *Geodin. Acta*, 29(1), 20–41.

Herdianita, N. R., Browne, P. R. L., Rodgers, K. A., and Campbell, K. A. (2000). Mineralogical and textural changes accompanying ageing of silica sinter. *Miner. Depo.*, 35(1), 48–62.

Hinman, N. W. and Walter, M. R. (2005). Textural preservation in siliceous hot spring deposits during early diagenesis: examples from Yellowstone National Park and Nevada, USA. *J. Sediment. Res.*, 75(2), 200–215.

Hoefs, J. (1987). *Stable Isotope Geochemistry*. Springer-Verlag, Berlin, Heidelberg, New York.

Ivanov, V. V., Barabanov, L. N., and Plotnikova, G. N. (1968). The main genetic types of the Earth's Crust mineral waters and their distribution in the USSR. In *International Geological Congress of 23rd Sessions Czechoslovakia*, volume 17, pages 33–39.

Jones, B. and Renaut, R. W. (2010). Calcareous spring deposits in continental settings. In: carbonates in continental settings: facies, environments, and processes. In Alonso Zarza, A. M. and Taner, L. H., editors, *Developments in Sedimentology*, volume 61, pages 177–224. Elsevier, Amsterdam.

Kanellopoulos, C. (2012). Distribution, lithotype and mineralogical study of newly formed thermogenic travertines in Northern Euboea and Eastern Central Greece. *Cent. Eur. J. Geosci.*, 4, 545–560.

Kanellopoulos, C., Mitropoulos, P., Valsami-Jones, E., and Voudouris, P. (2017). A new terrestrial active mineralizing hydrothermal system associated with ore-bearing travertines in Greece (northern Euboea Island and Sperchios area). *J. Geochem. Explor.*, 179, 9–24.

Kele, S., Özkul, M., Fórizs, I., Gökgöz, A., Baykara, M. O., Alcicek, M. C., and Nemeth, T. (2011). Stable isotope geochemical study of Pamukkale travertines: new evidences of low-temperature non-equilibrium calcite water fractionation. *Sediment. Geol.*, 238, 191–212.

Kronfeld, J., Vogel, J. C., Rosenthal, E., and Weinstein-Evron, M. (1988). Age and paleoclimatic implication of the Bet Shean travertine. *Quat. Res.*, 30, 298–303.

Lasserre, M. (1961). Étude géologique de la partie orientale de l'Adamaoua (Cameroun central). *Bull. Dir. Mines Géol. Camer.*, 4, 1–130.

Lasserre, M. (1962). Carte géologique du Cameroun à 1/500 000, coupure Ngaoundéré Est avec notice explicative. Dir. Géol. Mines du Cameroun.

Le Maréchal, A. (1976). *Géologie et Géochimie des Sources Thermo-Minérales du Cameroun*, volume 59. Travaux et documents de l'ORSTOM, Paris.

Le Maréchal, A. and Vincent, P. M. (1971). Le fossé crétacé du Sud-Adamaoua (Cameroun). *Cahier ORSTOM, Sér. Géol.*, 3(1), 67–83.

Lowe, D. R. and Braunstein, D. (2003). Microstructure of high–temperature (>73 °C) siliceous sinter deposits around hot springs and geysers, Yellowstone National Park: the role of biological and abiological processes in sedimentation. *Can. J. Earth Sci.*, 40(11), 1611–1642.

Magnin, F., Guendon, J. L., Vaudour, J., and Martin, P. (1991). Les travertins : accumulations carbonatées associées aux systèmes karstiques, séquences sédimentaires et paleoenvironnements quaternaires. *Bull. Soc. Géol. Fr.*, 162(3), 585–594.

Mancini, A., Della Porta, G., Swennen, R., and Capezzuoli, E. (2021). 3D reconstruction of the Lapis Tiburtinus (Tivoli, Central Italy): The control of climatic and sea-level changes on travertine deposition. *Basin Res.*, 33(5), 2605–2635.

Marzoli, A., Renne, P. R., Piccirillo, E. M., Francesca, C., Bellieni, G., Melfi, A. J., Nyobe, J. B., and N'ni, J. (1999). Silicic magmas from the continen-

tal Cameroon Volcanic Line (Oku, Bambouto and Ngaoundere): ^{40}Ar–^{39}Ar dates, petrology, Sr-Nd-O isotopes and their petrogenetic significance. *Contrib. Mineral. Petrol.*, 35, 133–150.

Matera, P. F., Ventruti, G., Zucchi, M., Brogi, A., Capezzuoli, E., Liotta, D., Yu, T. L., Shen, C. C., Huntington, K. W., Rinyu, L., and Kele, S. (2021). Geothermal fluid variation recorded by banded ca-carbonate veins in a fault-related, fissure ridge-type travertine depositional system (Iano, southern Tuscany, Italy). *Geofluids*, 2021, article no. 8817487.

McDonough, W. F. and Sun, S. S. (1995). The composition of the earth. *Chem. Geol.*, 120, 223–253.

McLennan, S. M. (2001). Relationships between the trace element compositions of sedimentary rocks and upper continental crust. *Geochem. Geophys. Geo-Syst.*, 2, 86–98.

Mesci, L. B., Gürsoy, H., and Tatar, O. (2008). The evolution of travertine masses in the Sivas Area (Central Turkey) and their relationships to active tectonics. *Turk. J. Earth Sci.*, 17, 219–240.

Minissale, A., Kerrick, D. M., Magro, G., Murrell, M. T., Paladini, M., Rihs, S., Sturchio, N. C., Tassi, F., and Vaselli, O. (2002). Geochemistry of quaternary travertines in the region north of Rome (Italy): structural, hydrologic and paleoclimatic implications. *Earth Planet. Sci. Lett.*, 203, 709–728.

Montigny, R., Ngounouno, I., and Deruelle, B. (2004). Ages K-Ar des roches magmatiques du fosse de Garoua (Cameroun) : leur place dans le cadre de la « Ligne du Cameroun ». *C. R. Geosci.*, 336, 1463–1471.

Moreau, C., Demaiffe, D., Bellion, Y., and Boullier, A. M. (1994). A tectonic model for the location of Paleozoic ring complexes in Aïr (Niger, West Africa). *Tectonophysics*, 94, 123–139.

Moreau, C., Regnoult, J. M., Deruelle, B., and Robineau, B. (1987). A new tectonic model for the Cameroon line, Central Africa. *Tectonophysics*, 139, 317–334.

Ngako, V., Njonfang, E., Aka, F. T., Affaton, P., and Nange, M. J. (2006). The North-South Paleozoic to Quaternary trend of alkaline magmatism from Niger-Nigeria to Cameroon: Complex interaction between hotspots and Precambrian faults. *J. Afr. Earth Sci.*, 45, 241–256.

Ngangom, E. (1983). Etude tectonique du fossé crétacé de la Mbere et du Djerem, Sud-Adamaoua, Cameroun. *Bull. Centres Rech. Explor. Product, Elf Aquitaine*, 7(1), 339–347.

Njike Ngaha, P. R. (1984). *Contribution à l'étude géologique, stratigraphique et structurale de la bordure du bassin atlantique au Cameroun.* Thèse 3ème cycle, Université de Yaoundé, Cameroun.

Ohmoto, H. and Rye, R. O. (1979). Isotopes of sulfur and carbon. In Barnes, H. L., editor, *Geochemistry of Hydrothermal Ore Deposits*, pages 509–567. John Wiley, New York.

Ollivier, V., Roiron, P., Balasescu, A., Nahapetyan, S., Gabrielyan, Y., and Guendon, J. L. (2009). Milieux, processus, facies et dynamiques morpho-sédimentaires des formations travertineuses quaternaires en relation avec les changements climatiques et les occupations humaines entre Méditerranée et Caucase. *Stud. Preistorie*, 5, 15–35.

Osmond, J. K. and Dabous, A. A. (2004). Timing and intensity of groundwater movement during Egyptian Sahara pluvial periods by U-series analysis of secondary U in ores and carbonates. *Quat. Res.*, 61, 85–94.

Parfenoff, A., Pomerol, Ch., and Tourenq, J. (1970). *Les minéraux en grains: Méthodes d'études et détermination.* Masson, Paris.

Pentecost, A. (1995). The quaternary travertine deposits of Europe and Asia Minor. *Quat. Sci. Rev.*, 14, 1005–1028.

Pentecost, A. (2005). *Travertine.* Springer Verlag, Berlin.

Pentecost, A. and Viles, H. (1994). A review of travertine classification. *Geogr. Phys. Quat.*, 48, 305–314.

Pola, M., Gandin, A., Tuccimei, P., Soligo, M., Deiana, R., Fabbri, P., and Zampieri, D. (2014). A multidisciplinary approach to understanding carbonate deposition under tectonically controlled hydrothermal circulation: a case study from a recent travertine mound in the euganean hydrothermal system, northern Italy. *Sedimentology*, 61, 172–199.

Renaut, R. W. and Jones, B. (2000). In *Microbial Precipitates Around Continental Hot Springs and Geysers. Microbial Sediments*, pages 187–195. Springer-Verlag, Berlin, Heidelberg.

Renaut, R. W. and Jones, B. (2011). Hydrothermal environments, terrestrial. In Reitner, J. and Thiel, V., editors, *Encyclopedia of Geobiology*, pages 467–479. Springer, Dordrecht, NL.

Renaut, R. W., Owen, R. B., and Ego, J. K. (2017). Geothermal activity and hydrothermal mineral de-

posits at southern Lake Bogoria, Kenya Rift Valley: Impact of lake level changes. *J. Afr. Earth Sci.*, 129, 623–646.

Rodgers, K. A., Browne, P. R. L., Buddle, T. F., Cook, K. L., Greatrex, R. A., Hampton, W. A., and Teece, C. I. A. (2004). Silica phases in sinters and residues from geothermal fields of New Zealand. *Earth Sci. Rev.*, 66(1–2), 1–61.

Rodríguez-Berriguete, A., Alonso-Zarza, A. M., Cabrera, M. C., and Rodriguez-Gonzalez, A. (2012). The Azuaje travertine: an example of aragonite deposition in a recent volcanic setting, North Gran Canaria Island, Spain. *Sediment. Geol.*, 277, 61–71.

Schinteie, R., Campbell, K. A., and Browne, P. R. L. (2007). Microfacies of stromatolitic sinter from acid–sulphate–chloride springs at Parariki stream, Rotokawa geothermal field, New Zealand. *Palaeontol. Electron.*, 10, 1–33.

Sillitoe, R. H. (1993). Epithermal models: genetic types, geometric controls and shallow features. In Kirkham, R. V., Sinclair, W. D., Thorpe, R. I., and Duke, J. M., editors, *Ore Deposits Modeling*, volume 40, pages 403–417. Geological Association of Canada, St Johns (NL).

Suh, C. E., Spark, R. S. J., Fitton, J. G., Ayongue, S. N., Annen, C., Nana, R., and Luckman, A. (2003). The 1999 and 2000 eruption of Mount Cameroon: eruption behavior and petrochemistry of lava. *Bull. Volcanol.*, 65, 267–281.

Tchameni, R., Pouclet, A., Penaye, J., Ganwa, A. A., and Toteu, S. F. (2006). Petrography and geochemistry of the Ngaoundéré Pan- African granitoids in central north Cameroon: Implications for their sources and geological setting. *J. Afr. Earth Sci.*, 44, 511–529.

Tchoua, F. (1974). Contribution à l'étude géologique et pétrologique de quelques volcans de la « ligne du Cameroun » (Monts Manengouba et Bambouto). p. 346.

Tchoua, F. (1977). Le travertin de Lobe. *Ann. Fac. Sci. Yaoundé*, 23–24, 59–63.

Tchouatcha, M. S. (2011). Les bassins du Mbere et du Djerem dans le contexte régional Sud Adamaoua : genèse, évolution stratigraphique et reconstitution des paléoenvironnements.

Tchouatcha, M. S., Kouske, A. P., Takojio Nguemo, R. E., Ganno, S., Kouonang Tchounang, S., Kono, L. D., Ngonlep Miyemeck, V. T., Fon Asah, M., and Ngong Njinchuki, D. (2018). The active thermogene travertine deposits along the Cameroon volcanic line (CVL), Central Africa: Petrology and insights for neotectonics and paleoenvironmental approach. *J. Afr. Earth Sci.*, 144, 1–16.

Tchouatcha, M. S., Njike Ngaha, P. R., Mahmoud, M. S., Deaf, A. S., and Ekodeck, G. E. (2010). Existence of « late continental » deposits in the Mbere and Djerem sedimentary basins (North Cameroon): palynologic and stratigraphic evidence. *J. Geol. Min. Res.*, 2(6), 159–169.

Tchouatcha, M. S., Njoya, A., Ganno, S., Toyama, R., Ngouem, P. A., and Njike Ngaha, P. R. (2016). Origin and paleoenvironmental of Pleistocene-Holocene travertine deposit from the Mbere sedimentary sub-basin along the Central Cameroon Shear Zone: Insights from petrology and palynology and evidence for neotectonics. *J. Afr. Earth Sci.*, 118, 24–34.

Tchuimegnie Ngongang, B. N., Kamgang, P., Chazot, G., Agranier, A., Bellon, H., and Nonnotte, P. (2016). Age, geochemical characteristics and petrogenesis of Cenozoic intraplate alkaline volcanic rocks in the Bafang region, West Cameroon. *J. Afr. Earth Sci.*, 102, 218–232.

Temdjim, R., Njilah, I. K., Kamgang, P., and Nkoumbou, C. (2004). Données nouvelles sur les laves felsiques de Ngaoundéré (Adamaoua, ligne du Cameroun) : chronologie K/Ar et pétrologie. *Afr. J. Sci. Technol.*, 5(2), 113–123.

Temdjim, R., Notsa Wamba, G. D., Njilah Konfor, I., and Hébert, V. (2010). Kélyphitisation des grenats des pyroxénites du Maar basaltique de Youkou, Ngaoundéré-Est (Adamaoua- Cameroun). *Ann. Fac. Sci.*, 1(38), 1–16.

Toker, E., Kayseri-Özer, M. S., Özkul, M., and Kele, S. (2015). Depositional architecture and palaeoclimatic dynamics of Late Pleistocene travertines: Kocabas, Denizli, SW Turkey. *Sedimentology*, 62, 1360–1383.

Turi, B. (1986). Stable isotope geochemistry of travertines. In Frit, P. and Fontes, P. J., editors, *Handbook of Environmental Isotopic Geochemistry*. Elsevier Science Publishers, Amsterdam.

Vignaroli, G., Berardi, G., Billi, A., Kele, S., Rossetti, F., Soligo, M., and Bernasconi, M. S. (2016). Tectonics, hydrothermalism, and paleoclimate recorded by Quaternary travertines and their spatio-temporal distribution in the Albegna basin, Central Italy: Insights on Tyrrhenian margin neotectonics. *Lithos*,

8(4), 335–358.

Wachter, E. A. and Hayes, J. M. (1985). Exchange of oxygen isotopes in carbon dioxide-phosphoric acid systems. *Chem. Geol.*, 52, 365–374.

Weisrock, A., Rousseau, L., Reyss, J. L., Falgueres, C., Ghaleb, B., Bahain, J. J., Beauchamp, J., Boudad, L., Mercier, N., Mahieux, G., Pozzi, J. P., Janati-Idrissi, N., and Ouammou, A. (2008). Travertins de la bordure nord du Sahara marocain : dispositifs morphologiques, datation U/Th et indications paléoclimatiques. *Géo. Relief Process. Environ.*, 14, 153–167.